



Experimental Test of Error-Disturbance Uncertainty Relations by Weak Measurement

Fumihiko Kaneda,^{1,*} So-Young Baek,^{1,†} Masanao Ozawa,² and Keiichi Edamatsu¹

¹Research Institute of Electrical Communication, Tohoku University, Sendai 980-8577, Japan

²Graduate School of Information Science, Nagoya University, Nagoya 464-8601, Japan

(Received 27 August 2013; published 15 January 2014)

We experimentally test the error-disturbance uncertainty relation (EDR) in generalized, strength-variable measurement of a single photon polarization qubit, making use of weak measurement that keeps the initial signal state practically unchanged. We demonstrate that the Heisenberg EDR is violated, yet the Ozawa and Branciard EDRs are valid throughout the range of our measurement strength.

DOI: 10.1103/PhysRevLett.112.020402

PACS numbers: 03.65.Ta, 03.67.-a, 42.50.Xa

The error-disturbance uncertainty relation (EDR) is one of the most fundamental issues in quantum mechanics since the EDR describes a peculiar limitation on measurements of quantum mechanical observables. In 1927, Heisenberg [1] argued that any measurement of the position Q of a particle with the error $\epsilon(Q)$ causes the disturbance $\eta(P)$ on its momentum P so that the product $\epsilon(Q)\eta(P)$ has a lower bound set by the Planck constant. The generalized form of the Heisenberg EDR for an arbitrary pair of observables A and B is given by

$$\epsilon(A)\eta(B) \geq C, \quad (1)$$

where $C = |\langle[A, B]\rangle|/2$, $[A, B] = AB - BA$, and $\langle \dots \rangle$ stands for the mean value in a given state. It should be emphasized that Eq. (1) is not equivalent to the following relation that is mathematically proven [2,3]:

$$\sigma(A)\sigma(B) \geq C, \quad (2)$$

where $\sigma(A) = \sqrt{\langle A^2 \rangle - \langle A \rangle^2}$ is the standard deviation. Indeed, the Heisenberg EDR (1) is derived from (2) under certain additional assumptions [4–9], but could fail where such assumptions are not satisfied.

In 2003, Ozawa [10] proposed an alternative EDR that is theoretically proven to be universally valid

$$\epsilon(A)\eta(B) + \epsilon(A)\sigma(B) + \sigma(A)\eta(B) \geq C. \quad (3)$$

The presence of two additional terms indicates that the first Heisenberg term $\epsilon(A)\eta(B)$ is allowed to be lower than C , violating Eq. (1). To derive Eq. (3), the error and disturbance were defined [10] for any general indirect measurement model depicted as a “measurement apparatus” (MA) in Fig. 1

$$\begin{aligned} \epsilon(A) &\equiv \langle [U^\dagger(I \otimes M)U - A \otimes I]^2 \rangle^{1/2}, \\ \eta(B) &\equiv \langle [U^\dagger(B \otimes I)U - B \otimes I]^2 \rangle^{1/2}, \end{aligned} \quad (4)$$

where the average is taken in the state $|\psi\rangle_s \otimes |\xi\rangle_p$ of the signal-probe composite system, U is a unitary operator that provides interaction between the signal and probe systems, and M is the meter observable in the probe to be directly observed. The definition of $\epsilon(A)$ is uniquely derived from the classical notion of root-mean-square error if $U^\dagger(I \otimes M)U$ and $A \otimes I$ commute [11], and otherwise, it is considered as a natural quantization of the notion of classical root-mean-square error (see Supplemental Material [12]). The definition of $\eta(B)$ is derived analogously, although there are recent debates on alternative approaches [11,13–17].

Most recently, Branciard [18] has improved the Ozawa EDR as

$$\left[\epsilon(A)^2\sigma(B)^2 + \sigma(A)^2\eta(B)^2 + 2\epsilon(A)\eta(B)\sqrt{\sigma(A)^2\sigma(B)^2 - C^2} \right]^{1/2} \geq C, \quad (5)$$

which is universally valid and tighter than the Ozawa EDR. Here $\epsilon(A)$ and $\eta(B)$ are still defined by Eq. (4). It is also pointed out [18] that the above relation becomes even stronger for spin measurements as described later.

For experimental testing of EDRs, so far, two methods have been proposed: One is the so-called “three-state method” [9], in which $\epsilon(A)$, for instance, is obtained through the measurements of M on the prepared signal states, $|\psi\rangle_s$, $A|\psi\rangle_s$, and $(A + I)|\psi\rangle_s$, as shown in Fig. 1(a). The three-state method was demonstrated in recent experimental tests of EDRs for qubit systems: projective measurement of a neutron-spin qubit [19,20] and generalized measurement of a photon-polarization qubit [21]. The other method is called the “weak-probe method” [22,23]. The three-state method is simpler to implement for a single qubit system, but the weak-probe method is more feasible in a general case. In this method, as shown in Fig. 1(b), a “weak probe” (WP) measures A or B with a weak measurement strength prior to the main measurement operated by the MA. When the

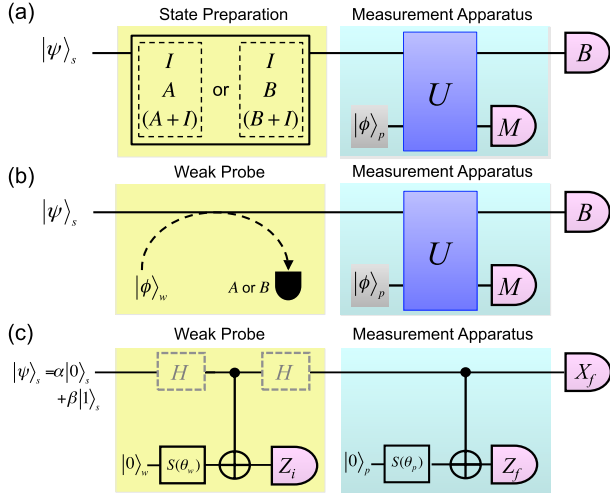


FIG. 1 (color online). Schematic diagram to test error-disturbance relation using (a) three-state method and (b) weak-probe method. (c) Quantum circuit model of the weak-probe method for single-qubit observables $A = M = Z$ and $B = X$.

measurement strength is sufficiently small, the signal state is sent to the MA without being disturbed by the WP. As Lund and Wiseman [22], and Ozawa [23] pointed out, the error (disturbance) defined by Eq. (4) is given by the “weak-valued root-mean-square difference” between measurement outcomes of the WP and the MA (postmeasurement of B)

$$\begin{aligned}\epsilon(A)^2 &= \sum_{i,f} (a_i - a_f)^2 P_{wv}(a_i, a_f), \\ \eta(B)^2 &= \sum_{i,f} (b_i - b_f)^2 P_{wv}(b_i, b_f),\end{aligned}\quad (6)$$

where $P_{wv}(a_i, a_f)$ is the weak-valued joint probability distribution [24,25] taking the outcomes a_i in the WP and a_f in the MA. As described later, we can experimentally estimate $P_{wv}(a_i, a_f)$, and thus $\epsilon(A)$, by evaluating the probability distribution $P(a_i, a_f)$ that we take the outcomes a_i and a_f . Similarly, $\eta(B)$ is given by $P_{wv}(b_i, b_f)$ taking outcomes b_i in the WP and b_f in the postmeasurement of B .

Recently, Rozema *et al.* [26] demonstrated the experimental test of EDRs for a single-photon polarization measurement using the weak-probe method. They used a pair of entangled photons, one for a signal qubit subjected to the main measurement and the other for an ancillary qubit subjected to the weak-probe measurement. The state of the ancillary qubit after the weak-probe measurement was then “teleported” onto the signal qubit and subjected to the main measurement. Although this fascinating scheme did work, in a real experiment it was rather complicated; imperfect teleportation fidelity and rather strong measurement strength used for the WP resulted in a considerable amount of disturbance on the system state. As a consequence, the

rhs of the EDR was decreased to $C \sim 0.8$ [26] from its ideal value $C = 1$.

In this Letter, we report the experimental test of the EDR for a single-photon polarization measurement using the weak-probe method. Our experiment uses only linear optical devices and single photons without entanglement, in a straightforward manner to the original proposal by Lund and Wiseman [22]. Another advantage of our design is that it provides in principle no loss apparatuses for the WP and MA, unlike lossy apparatuses used in the previous experiment [26]. With this simple implementation, we can use sufficiently weak measurement strength for the WP that causes very little disturbance on the signal state. We show that our results clearly violate the Heisenberg EDR, yet validate both the Ozawa [10] and Branciard [18] relations.

Our optical implementation of the weak-probe method is based on the quantum circuit model [22] depicted in Fig. 1(c). We take the signal observable to be measured as $A = Z$ and $B = X$, where X, Y , and Z denote the Pauli matrices, and $\{|0\rangle, |1\rangle\}$ are the eigenbasis of Z with the eigenvalues of $\{1, -1\}$. The postmeasurement observable for X is X_f , and the probe observable in the MA and WP are Z_f and Z_i , respectively. Then, we use the following notation as the measurement outcomes: $a_{i,f} = z_{i,f} = \pm 1$ and $b_{i,f} = x_{i,f} = \pm 1$. We employ two cascaded circuits as the WP and MA; both circuits work in the same manner. In the MA, the probe qubit initialized to $|0\rangle_p$ is rotated by $S(\theta) = \begin{pmatrix} \cos \theta & \sin \theta \\ \sin \theta & -\cos \theta \end{pmatrix}$, where $0 \leq \theta \leq \pi/4$. Then, the probe qubit is subjected to a controlled-NOT (CNOT) operation with the signal qubit. The positive operator valued measure (POVM) elements corresponding to the outcomes of $z_f = \pm 1$ are [21]

$$\Pi_{z_f=\pm 1} = \frac{1}{2}[I \pm (\cos 2\theta)Z]. \quad (7)$$

Here, $\cos 2\theta$ is the “measurement strength” of the MA. By changing $\cos 2\theta$ from 0 to 1, $\Pi_{z_f=\pm 1}$ change from identity (no measurement) to projector (strong measurement). The WP works in exactly the same manner as the MA except that the measurement strength of the WP is $\cos 2\theta_w$. In order to keep the WP’s measurement strength sufficiently weak, θ_w should be close to $\pi/4$. In addition, two Hadamard gates (H) are inserted to the signal qubit before and after the CNOT in the WP when weak measurement for X is taken.

The experimental setup to test the EDR by the weak-probe method is illustrated in Fig. 2(a). In our experiment, horizontal and vertical polarizations, $|H\rangle$ and $|V\rangle$, of a single photon are chosen as the signal qubit with eigenstates $|0\rangle$ and $|1\rangle$ of Z , respectively. Thus, the measurement in the MA corresponds to the polarization measurement in the H - V basis and does the postmeasurement of X to the $\pm 45^\circ$ linear polarization basis. In this apparatus, the

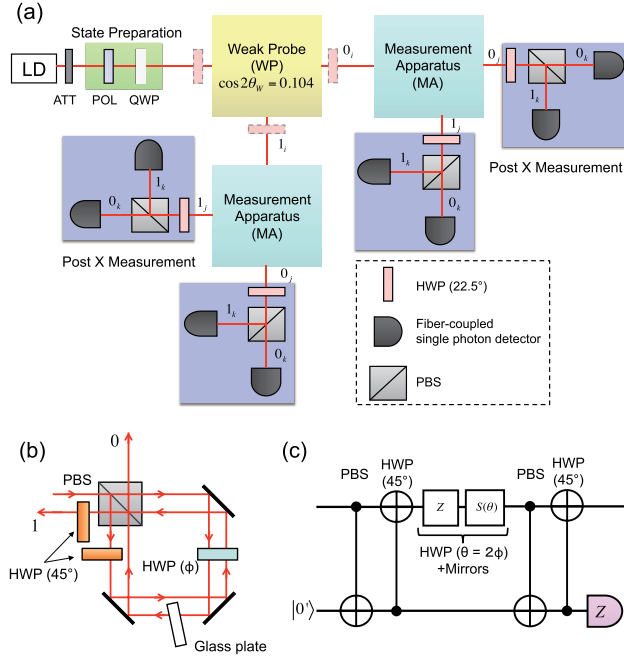


FIG. 2 (color online). (a) Schematic diagram of the experimental setup. Our optical implementation is separated into the state preparation, WP, MA, and post X measurement. In these apparatuses, our signal qubit is the polarization state of a photon, and the path degree of freedom of the same photon is the probe qubit; each apparatus has two output paths (0 or 1) corresponding to the measurement outcomes. For the weak measurement of X , additional HWPs (dashed rectangles) are inserted on both sides of the WP. The WP and MA are based on the polarization-division Sagnac interferometer (b) and the corresponding quantum circuit is depicted in (c), where the quantum operations of the PBS, HWPs, and mirrors are indicated (see Supplemental Material [12]). The glass plate compensates the phase difference between the two counter-propagating paths.

probe qubit is the path degree of freedom of the same photon; the two output paths correspond to the two possible outcomes of the probe qubit. Thus, we need two MAs after the WP and two post X measurement apparatuses after each MA. Figure 2(b) illustrates our optical implementation of the WP and MA which are based on the idea of a variable polarization beam splitter [27,28,21]. In the present experiment, we employed the displaced Sagnac configuration [29] that provides much higher phase stability than the Mach-Zehnder configuration used in our previous experiment [21]. The corresponding quantum circuit of our instrument is shown in Fig. 2(c), which provides the same POVM as that of Fig. 1(c) when the initial probe state is $|0\rangle_p$ (see Supplemental Material [12]). For the WP and X postmeasurement, we use polarization beam splitters (PBSs) with $e_r \approx 100$ and $e_t > 10^3$, where e_r and e_t are the PBS reflection extinction ratio and transmission extinction ratio [21], respectively. For the PBSs used in the MA, $e_r \approx 50$ and $e_t > 10^3$.

As a photon source, we used a continuous-wave diode laser (LD) whose center wavelength was at 686 nm, and the laser power was strongly attenuated by an attenuator (ATT) so that the mean photon number existing in the whole apparatus at a time was ~ 0.002 . Although we used a faint coherent state instead of a single-photon state as the input, the expected result is the same regardless of the photon statistics because the apparatus consists of linear optics and single-photon detection. To take the most stringent test of the Ozawa and Heisenberg EDRs, we chose the signal state as $|\psi_0\rangle_s = (|H\rangle + i|V\rangle)/\sqrt{2}$, an eigenstate of Y , so that the rhs of the EDRs become the maximum value in the qubit measurement; $C = |\langle[Z, X]\rangle|/2 = |\langle Y\rangle| = 1$. We used a polarizer (POL) and a quarter-wave plate (QWP) to prepare the signal qubit in $|\psi_0\rangle_s$. A half-wave plate (HWP) rotated at 22.5° worked as a Hadamard gate for polarization qubits, rotating the photon's polarization by 45° . The HWPs before and after the WP changed the measurement basis of the WP, between Z and X . In the experiment, the measurement strength of the WP was set to $\cos 2\theta_w = 0.104$ that produced a very small disturbance in the initial signal state; we expected $C = 0.995$, which was close to the ideal value $C = 1$. Then, the signal photon was subjected to the MA. Because the WP had two output outcomes, we put two identical MAs after the WP. At each output port of the MA, we put an instrument for the X postmeasurement, consisting of a HWP, PBS, and two photon counting detectors. We recorded the photon counting events N_{ijk} in the single-photon detectors, where the subscript $i, j, k = 0, 1$ denotes the outcomes of the WP, MA, and X postmeasurement, respectively. From Eq. (6) and the expression of weak-valued joint probability distribution [22], $\epsilon(Z)$ is given by

$$\epsilon(Z)^2 = 2 \left(1 - \frac{1}{\cos \theta_w} \sum_{z_i, z_f} z_i z_f P(z_i, z_f) \right), \quad (8)$$

where $P(z_i, z_f)$ is the joint probability distribution taking the outcomes z_i in the WP and z_f in the MA. Note that $\cos \theta_w$ is the measurement strength of the WP. $\eta(X)$ is given by simply replacing z_i and z_f with x_i and x_f , respectively. To evaluate $\epsilon(Z)$ and $\eta(X)$ using Eq. (8), we experimentally obtain $P(z_i, z_f)$, and $P(x_i, x_f)$, analyzing the statistics of the single photon counting rates N_{ijk} of the eight single-photon detectors. For instance, $P(z_i = 1, z_f = 1) = \sum_k N_{00k} / \sum_{i,j,k} N_{ijk}$.

Thus, the quantities of $\epsilon(Z)$ and $\eta(X)$ obtained are shown in Fig. 3(a). The error bars are obtained by rms of repeated measurements for ten times. The dashed curves represent the theoretical calculations of $\epsilon(Z)$ and $\eta(X)$ assuming the ideal instrument shown in Fig. 1(c), and the solid curves are those in which the imperfect extinction ratio of the PBS is taken into account (detailed discussion is given in Refs. [22,21]). The experimentally measured error and disturbance present good agreement with the theoretical calculations. A small amount of systematic deviation from the calculation might originate from additional experimental imperfections that

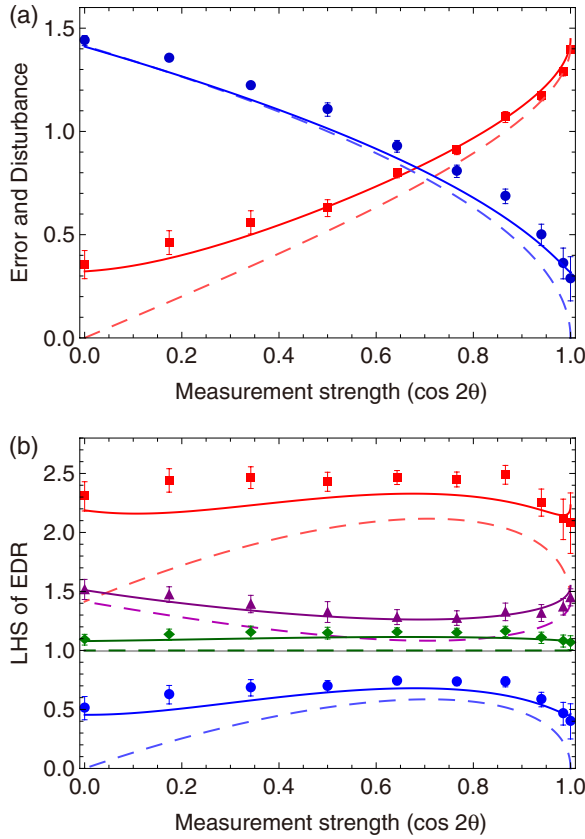


FIG. 3 (color online). Experimental results. (a) The error $\epsilon(Z)$ (blue circles) and disturbance $\eta(X)$ (red squares) as functions of the measurement strength $\cos 2\theta$. Dashed curves are the theoretically calculated error and disturbance for perfect implementation of the quantum circuit presented in Fig. 1(c). Solid curves are the theoretical values after the nonideal extinction ratio of a PBS is taken into account. (b) Left-hand sides of the EDRs. Blue circles: the Heisenberg EDR in Eq. (1). Red squares: the Ozawa EDR in Eq. (3). Purple triangles: the Branciard EDR in Eq. (5). Green diamonds: the Branciard EDR in Eq. (9). Dashed and solid curves are plotted in the same way as (a). The right-hand side of the EDRs ($C = 0.995$) is indicated by the gray line, which is nearly overlapped by the dashed green curve.

are not fully understood yet. Nevertheless, we clearly see the trade-off relation between the error and disturbance; as the measurement strength increases, $\epsilon(Z)$ decreases while $\eta(X)$ increases. The experimental error and disturbance remain finite even when the other goes to zero in the ideal case, since the error and disturbance are given by rms difference between ± 1 -valued observables.

From the experimentally measured error and disturbance, we evaluate the quantities of the lhs of the EDRs. We plot the lhs of the Heisenberg EDR [Eq. (1), blue], the Ozawa EDR [Eq. (3), red], and the Branciard EDR [Eq. (5), purple], as shown in Fig. 3(b). Also plotted is the stronger Branciard EDR (green) that is applicable to the case (including ours) where the system and probe observables are both ± 1 valued and $\langle A \rangle = \langle B \rangle = 0$ [hence $\sigma(A) = \sigma(B) = 1$] [18]

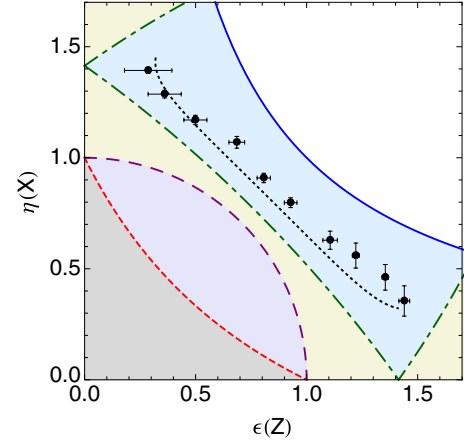


FIG. 4 (color online). Comparison of EDRs' lower bounds in the error-disturbance plot. Blue (solid) curve: the Heisenberg bound in Eq. (1). Red (short dashed) curve: the Ozawa bound in (3). Purple (long dashed) curve: the Branciard bound in (5). Green (dotted-dashed) curve: the Branciard bound in (9). Black (filled) circles: experimental data shown in Fig. 3(a). Black (dotted) curve: theoretical prediction for our experiment using imperfect PBSs. The lower-left side of each bound is the forbidden region by the corresponding EDR. Each bound was calculated for $C = 1$.

$$\left[\tilde{\epsilon}(A)^2 + \tilde{\eta}(B)^2 + 2\tilde{\epsilon}(A)\tilde{\eta}(B)\sqrt{1-C^2} \right]^{1/2} \geq C, \quad (9)$$

where $\tilde{\epsilon} = \epsilon\sqrt{1-\epsilon^2/4}$ and $\tilde{\eta} = \eta\sqrt{1-\eta^2/4}$. The solid and dashed curves are the theoretical predictions for each EDR with and without the imperfect extinction ratio of the PBS taken into account. In our experiment, the rhs of the EDRs is $C = 0.995$, which is indicated by the gray line. Our experimental results demonstrate the clear violation of the Heisenberg EDR, while the Ozawa and Branciard EDRs are always satisfied throughout the range of our measurement strength. We see that the Branciard EDRs are stronger than the Ozawa EDR; they are closer to the lower bound C than that of Ozawa. In particular, the lhs of Eq. (9) saturates to the lower bound ($C = 1$) for the ideal case. Our results exhibit near saturation to the lower bound, when experimental imperfection originating from nonideal PBSs is taken into account. In this experimental demonstration of the new, stronger EDR, the use of weak measurement with sufficiently weak measurement strength is essential. It is also noteworthy that the experimental results are consistent with those reported in Ref. [21] in which we used a similar apparatus and the three-state method to test the Heisenberg and Ozawa EDRs.

In Fig. 4, we plot the predicted lower bounds of the EDRs in Eqs. (1), (3), (5), and (9), together with the experimental data. Under the Heisenberg EDR, the error or disturbance must be infinite when the other goes to zero, while other EDRs allow a finite error or disturbance even when the other is zero. Again, we see that the experimental data violate the Heisenberg EDR, yet satisfy the Ozawa and Branciard EDRs. Our experimental data were close to

the Branciard bound (dotted-dashed curve) given in Eq. (9), which could be saturated by ideal experiments.

In conclusion, we have experimentally tested the Heisenberg, Ozawa, and Branciard EDRs in generalized photon polarization measurements making use of weak measurement that keeps the initial signal state practically unchanged. Our experimental results clearly demonstrated that the Ozawa and Branciard EDRs were valid, but that the Heisenberg EDR was violated throughout the range of the measurement strength (from no measurement to projective measurement). In particular, our results demonstrated near saturation to the lower bound of the stronger Branciard EDR. Such experimental investigation of the EDRs will be of demanded importance not only in understanding fundamentals of physical measurement but also in developing, for instance, novel measurement-based quantum information and communication protocols.

The authors thank C. Branciard for valuable discussion. This work was supported by MIC SCOPE No. 121806010 and the MEXT GCOE program. M.O. is supported by the John Templeton Foundations ID No. 35771 and the JSPS KAKENHI No. 21244007.

Note added.—Recently, we became aware of a related work by M. Ringbauer *et al* [30].

*Present address: Department of Physics, University of Illinois, Urbana-Champaign, IL 61801, USA.

†Present address: Department of Electrical and Computer Engineering, Duke University, Durham, NC 27708, USA.

- [1] W. Heisenberg, *Z. Phys.* **43**, 172 (1927).
- [2] E. H. Kennard, *Z. Phys.* **44**, 326 (1927).
- [3] H. P. Robertson, *Phys. Rev.* **34**, 163 (1929).
- [4] E. Arthurs and M. S. Goodman, *Phys. Rev. Lett.* **60**, 2447 (1988).
- [5] M. G. Raymer, *Am. J. Phys.* **62**, 986 (1994).
- [6] M. Ozawa, *Lect. Notes Phys.* **378**, 1 (1991).
- [7] S. Ishikawa, *Rep. Math. Phys.* **29**, 257 (1991).
- [8] M. Ozawa, *Phys. Lett. A* **318**, 21 (2003).
- [9] M. Ozawa, *Ann. Phys. (Amsterdam)* **311**, 350 (2004).
- [10] M. Ozawa, *Phys. Rev. A* **67**, 042105 (2003).
- [11] M. Ozawa, [arXiv:1308.3540](https://arxiv.org/abs/1308.3540).
- [12] See Supplemental Material at <http://link.aps.org/supplemental/10.1103/PhysRevLett.112.020402> for the definitions of measurement error and disturbance, the modeling of apparatus, and the experimental details.
- [13] P. Busch, T. Heinonen, and P. Lahti, *Phys. Rep.* **452**, 155 (2007).
- [14] Y. Watanabe, T. Sagawa, and M. Ueda, *Phys. Rev. A* **84**, 042121 (2011).
- [15] M. M. Weston, M. J. W. Hall, M. S. Palsson, H. M. Wiseman, and G. J. Pryde, *Phys. Rev. Lett.* **110**, 220402 (2013).
- [16] P. Busch, P. Lahti, and R. F. Werner, *Phys. Rev. Lett.* **111**, 160405 (2013).
- [17] L. A. Rozema, D. H. Mahler, A. Hayat, and A. M. Steinberg, [arXiv:1307.3604](https://arxiv.org/abs/1307.3604).
- [18] C. Branciard, *Proc. Natl. Acad. Sci. U.S.A.* **110**, 6742 (2013).
- [19] J. Erhart, S. Sponar, G. Sulyok, G. Badurek, M. Ozawa, and Y. Hasegawa, *Nat. Phys.* **8**, 185 (2012).
- [20] G. Sulyok, S. Sponar, J. Erhart, G. Badurek, M. Ozawa, and Y. Hasegawa, *Phys. Rev. A* **88**, 022110 (2013).
- [21] S.-Y. Baek, F. Kaneda, M. Ozawa, and K. Edamatsu, *Sci. Rep.* **3**, 2221 (2013).
- [22] A. P. Lund and H. M. Wiseman, *New J. Phys.* **12**, 093011 (2010).
- [23] M. Ozawa, *Phys. Lett. A* **335**, 11 (2005).
- [24] A. M. Steinberg, *Phys. Rev. Lett.* **74**, 2405 (1995).
- [25] H. M. Wiseman, *Phys. Lett. A* **311**, 285 (2003).
- [26] L. A. Rozema, A. Darabi, D. H. Mahler, A. Hayat, Y. Soudagar, and A. M. Steinberg, *Phys. Rev. Lett.* **109**, 100404 (2012).
- [27] S.-Y. Baek, Y. W. Cheong, and Y.-H. Kim, *Phys. Rev. A* **77**, 060308(R) (2008).
- [28] Y.-H. Kim, *Phys. Rev. A* **67**, 040301(R) (2003).
- [29] T. Nagata, R. Okamoto, J. L. O'Brien, K. Sasaki, and S. Takeuchi, *Science* **316**, 726 (2007).
- [30] M. Ringbauer, D. N. Biggerstaff, M. A. Broome, A. Fedrizzi, C. Branciard, and A. G. White, preceding Letter, *Phys. Rev. Lett.* **112**, 020401 (2014).